International Astronomy and Astrophysics Research Journal

2(4): 48-73, 2020; Article no.IAARJ.62848

Exploring Effect of Perturbing Forces on Periodic Orbits in the Restricted Problem of Three Oblate Spheroids with Cluster of Material Points

Oni Leke[1*] and Jagadish Singh[2]

[1]Department of Mathematics, Statistics and Computer Science, College of Science, University of Agriculture, P. M. B. 2373, Makurdi, Benue-State, Nigeria.
[2]Department of Mathematics, Faculty of Physical Science, Ahmadu Bello University Zaria, Kaduna State, Nigeria.

Authors' contributions

The author OL carried out all mathematical and numerical analysis and plotted all the graphs while the author JS made corrections to the manuscripts and supervised the work. Both authors read and approved the final manuscript.

Article Information

Editor(s):
(1) Dr. David Garrison, University of Houston-Clear Lake, Texas.
Reviewers:
(1) Bogning Jean Roger, University of Bamenda, Cameroon.
(2) Kumari Ranjana, University of Delhi, India.
(3) Volodymyr Krasnoholovets, Institute of Physics, Ukraine.
Complete Peer review History: http://www.sdiarticle4.com/review-history/62848

Original Research Article

Received 01 October 2020
Accepted 05 December 2020
Published 12 February 2021

ABSTRACT

This paper explores effect of perturbing forces on periodic orbits generated by the triangular equilibrium points of the restricted three-body problem taking into account small perturbations in the Coriolis and centrifugal forces when the infinitesimal mass is an oblate spheroid and the central binary is two radiating oblate stars surrounded by circular cluster of materials. We compute explicitly expressions for the frequency, angle of rotation of the principal axis, eccentricity and lengths of semi-major and minor axes of the orbits. Since some facts are not directly observable from the analytic solutions, numerical evidences are provided to analyze the structure and effect of each perturbing forces on the elements of the orbits. Among these, it is seen that the presence of cluster of materials reduces lengths of the semi-axes and is the only force that reduces the eccentricity while radiation pressure and oblateness of the primary star have same effect on the structure of the

**Corresponding author: E-mail: lekkyonix4ree@yahoo.com;*

orbits. Our study has relevance in the long-term motion of planets in binary systems, where planets have masses infinitesimally small. A question of celestial mechanics is how long can the triangular equilibrium points keep the infinitesimal mass in orbit from escaping? The determination of ranges of semi-major axis taking into account the perturbing forces may help to know if body is likely to remain or escape. It is seen that under combined effect of radiation, perturbations, oblateness and cluster of materials, the period, angle of rotation, eccentricity and length of semi-major axis all increases. Consequently, the infinitesimal mass is likely to escape in this case. However, with increasing accumulation of materials, the departure of the infinitesimal mass in orbit away from the vicinity of triangular equilibrium points is unlikely as it will override other perturbing forces and reduce the length of the semi-major axis.

Keywords: RTBP; periodic orbit; perturbing forces, triangular equilibrium points.

1. INTRODUCTION

Three-body problem is an important problem in the classical and quantum mechanics which involves modeling the motion of three particles subject to their mutually gravitational attractions. The simplest form of the three-body problem is the restricted three-body problem (RTBP). This formulation is the most searched and interesting problem for astrophysicists and the model describes the motion of an infinitesimal mass moving under the gravitational influence of two massive bodies called the primaries which move in circular orbits around their common center of mass on the account of their mutual attraction [1,2]. To tackle the problem of classical RTBP, Lagrange considered the behavior of the distances between the bodies without finding a general solution. He discovered two distinct classes of constant-pattern solutions in rotating frame of reference where gravitational equilibrium can be maintained. These points are called equilibrium points $L_i\left(i=1,2..5\right)$ and are very important in space missions [3]. The Solar and Hemispheric Observatory (SOHO) lunched in 1995 and Microwave Anisotropy Probe (MAP) lunched in 2001 by NASA are currently in operation at Sun-Earth collinear equilibrium points. Solar Terrestrial RElations Observatory-Ahead (STEREO-A) made its closest pass to triangular equilibria L_5 recently, on its orbit around the Sun. Also, Asteroid 2010 SO16 is currently proximal to L_5 point though at a high inclination (Smarandache & Christianto, 2006).

In view of the importance of equilibrium points to the exploration and development of space, among the most fundamental questions about motion near equilibrium points are those about the existence of periodic orbits. Therefore, it is imperative to study the periodic structures around equilibrium points due to the rotational motion. Elements that could be used to describe the motion of the infinitesimal mass relative to the primary and secondary bodies are categorized as orbital and non orbital elements [4]. Angular momentum and total energy are the integrals available to measure the shapes and sizes of the orbits but are not directly observable. Therefore, eccentricities, inclination and semi major axis of the orbits are used to determine the shapes, orientation and sizes of the orbits. Periodic orbits are also used as reference orbits. The study of periodic orbits is a very useful tool for the study of non-integrable dynamical system, because they determine critically the structure of phase space, while the study of periodic orbits, which are close to actual motions, plays an important role in the understanding of the general properties of such a system. Through the study of periodic orbits, one can understand the role of other forces besides gravitational forces. Szebehely's [3] gives a fairly good idea about the periodic orbits.

Many Mathematicians and astronomers have investigated periodic orbits of the RTBP under different assumptions. Zagouras [5] considered the effect of radiation pressure on the periodic motion of small particle in the vicinity of the triangular points. Elipe and Lara [6] discussed periodic orbits in the RTBP by taking both the primaries as the source of radiation pressure. By means of some modifications to the method of numerical continuation of natural family of periodic orbits, they found several families of periodic orbits, both in two and three dimensions. Perdios [7] studied critical symmetric periodic orbits in the photogravitational RTBP in which the first primary is a source of radiation, and the study was extended by Perdios and Kalantonis [8] when the first primary is an oblate spheroid. The investigation of the combined effect of perturbations, radiation and oblateness, on the periodic orbits in the neighborhood of linearly

stable triangular equilibrium points was carried out by Abdul Raheem and Singh [9]. The periodic orbits generated by Lagrangian solutions of the RTBP when one of the primaries is an oblate body, was studied by Mittal et al. [10] while Abouelmagd and El–Shaboury [11] studied periodic orbits around the triangular points when the three bodies are oblate spheroids and the primaries are radiating. Singh and Haruna [12] examined the periodic orbits around triangular points of three oblate bodies under effect of radiation pressure of the primaries and small perturbations in the Coriolis and centrifugal forces. Singh and Leke [13] studied the periodic orbits when the main masses in the system are surrounded by a cluster of particles. Later, Singh and Leke [14] investigated the periodic orbits of a test particle around triangular equilibrium points in the RTBP with variable masses. Palacios et al. [15] investigated the symmetric periodic orbits in the Moulton-Copenhagen problem while the locations of Lagrangian points and periodic orbits around triangular points in the photo gravitational elliptic RTBP with oblateness, was studied by Johnson and Sharma [16]. Recently, Mittal et al. [17] extended an earlier contribution of Mittal et al. [17] by studying the periodic orbits generated by the Lagrangian solutions of the RTBP when both primaries are oblate spheroids.

Inspired by the works of Singh and Haruna [12] and Singh and Leke [13], our aim in the present paper is to investigate effect of the perturbing forces on the periodic orbits around triangular equilibrium points of the restricted problem of three oblate bodies when the primaries are radiating stars and surrounded by a circular cluster of materials coupled with effect of small perturbations in the Coriolis and centrifugal forces. This paper can be viewed as an extension of the works of Abouelmagd and El–Shaboury [11] and that of Singh and Haruna [12].

The paper is organized in the following order: Section 2, contains the description of the equations of motion and locations of the triangular equilibrium points. Section 3 deals with the study of the periodic orbits. Here, the frequency and orientation of the elliptic orbits are computed both analytically and numerically. Numerical estimations of the period and periodic terms are also computed in this section and the orbits are drawn to show effect of the perturbing forces. In section 4, the eccentricity and length of the semi-major and minor axes of the elliptic orbits, are presented. The analytic computations have equally been backed up with numerical estimations. The discussion of our results is given in section 5 and conclusion drawn in section 6.

2. EQUATIONS OF MOTION AND TRIANGULAR EQUILIBRIUM POINTS

Let m_1 and m_2 be the masses of two radiating stars and let m_3 be the mass of the infinitesimal body. We assume that the three bodies are oblate spheroids and the stars are surrounded by a cluster of materials. Following the works of Singh and Haruna [12] and Singh and Leke [13], the governing equations of motion under perturbing forces of radiation pressure, oblateness of the bodies, Coriolis and centrifugal perturbations coupled with the gravitational potential from cluster of materials around the stars, have the form:

$$\begin{aligned} \ddot{x} - 2\varphi n\dot{y} &= U_x \\ \ddot{y} + 2\varphi n\dot{x} &= U_y \end{aligned} \tag{1}$$

where

$$U = \frac{n^2\psi\left(x^2+y^2\right)}{2} + \frac{q_1(1-\mu)}{r_1} + \frac{q_2\mu}{r_2} + \frac{\alpha_1 q_1(1-\mu)}{2r_1^3} + \frac{\alpha_2 q_2\mu}{2r_2^3} + \frac{\alpha_3(1-\mu)}{2r_1^3} + \frac{\alpha_3\mu}{2r_2^3} + \frac{M_d}{\left(r^2+T^2\right)^{1/2}}$$

$$n^2 = 1 + \frac{3}{2}\left(\alpha_1+\alpha_2\right) + \frac{2M_d r_c}{\left(r_c^2+T^2\right)^{3/2}} \tag{2}$$

$r_1^2 = (x-\mu)^2 + y^2, r_2^2 = (x-\mu+1)^2 + y^2$, $\alpha_i = \frac{AE_i^2 - AP_i^2}{5R^2}, \alpha_i << 1 : (i = 1,2,3)$.

q_1, q_2 are radiation pressures of the primary and secondary star, respectively, while α_1, α_2 and α_3 are the oblateness of the bodies of mass m_1, m_2 and m_3, respectively. r_1 and r_2 are the distances of the infinitesimal mass from the respective stars. The last term in U is the gravitational potential due to the mass M_d of the enclosed cluster of circular materials and $r = \sqrt{x^2 + y^2}$ is the radial distance of the infinitesimal mass, while $T = a + b$ defines the density profile of the accumulated materials. μ is the mass parameter and n is the mean motion of the stars while φ and ψ represent parameters through which small perturbations $\in$ and $\in'$ are given in the Coriolis and centrifugal forces, respectively such that $\varphi = 1 + \in, \psi = 1 + \in', |\in|, |\in'| << 1$ and $\in'$. R is the distance between the stars and, AE_i^2 and $AP_i^2 (i = 1,2,3)$ are the equatorial and polar radii of the bodies $m_i (i = 1,2,3)$, respectively.

Equations of motion (1), admits the Jacobi integral

$$C + (\dot{x}^2 + \dot{y}^2) = 2U \tag{3}$$

where C is the Jacobi constant.

The triangular points are the solutions of system (1) when the components of velocity and acceleration are zero and $y \neq 0$. Solving these equations, we get

$$x = \mu - \frac{1}{2} + \frac{1}{\psi^{2/3}}\left[\frac{1}{3}(1-q_1) - \frac{1}{3}(1-q_2) - \frac{1}{2}(\alpha_1 - \alpha_2)\psi^{2/3}\right] \tag{4}$$

$$y = \pm\frac{\sqrt{4-\psi^{2/3}}}{2\psi^{1/3}}\left\{1 - \frac{2}{4-\psi^{2/3}}\left[\frac{1}{3}(1-q_1) + \frac{1}{3}(1-q_2) + \frac{1}{2}(\alpha_1 + \alpha_2)(2-\psi^{2/3}) - \alpha_3\psi^{2/3} + \frac{2M_d(2\psi r_c - 1)}{3\psi(r_c^2 + T^2)^{3/2}}\right]\right\}$$

Equations (4) are the coordinates of the triangular equilibrium points of the problem of three oblate bodies under radiation pressure of the stars, small change in the Coriolis and centrifugal forces when the central binary is enclosed by a cluster of materials. The coordinates (4) differ from those in Singh and Haruna [12] only because of the last term in the $y-$ coordinate.

3. THE PERIODIC ORBITS

A dynamical system is periodic if the same configuration is repeated at regular intervals of time. Angular momentum and total energy are the integrals available to measure the shapes and sizes of the orbits but are not directly observable. Therefore, eccentricities, inclination and semi major axes of the orbits are used to determine the shapes, orientation and sizes of the orbits. In this section, we calculate the frequency, orientation, eccentricity and lengths of the semi-axes.

3.1 Angular Frequency of the Periodic Orbits

The characteristic equation when the infinitesimal mass is displaced away from the triangular equilibrium point is given as

$$\lambda^4+\left[4-3(\psi-1)+6(\alpha_1+\alpha_2)+8(\varphi-1)-3\left\{1+\frac{1}{2}(5-2\mu)\alpha_1+\frac{1}{2}(3+2\mu)\alpha_2+\alpha_3+\frac{(2\psi r_c-1)M_d}{\psi\left(r_c^2+T^2\right)^{3/2}}\right.\right.$$

$$\left.\left.+\frac{M_d\mu^2}{\psi\left(r_c^2+T^2\right)^{3/2}}-\frac{M_d\mu}{\left(r_c^2+T^2\right)^{3/2}}+\frac{M_d}{\left(r_c^2+T^2\right)^{3/2}}\right\}\right]\lambda^2+\frac{3}{4}\mu(1-\mu)\left[9+39(\alpha_1+\alpha_2)+12\alpha_3+22(\psi-1)\right.$$

$$\left.+2(1-q_1)+2(1-q_2)+\frac{M_d}{\left(r_c^2+T^2\right)^{3/2}}\left\{\frac{9}{\left(r_c^2+T^2\right)}+\frac{22}{\psi}(2\psi r_c-1)\right\}\right]=0 \qquad (5)$$

The four roots $\lambda_{1,2}=\pm i\omega_1$ and $\lambda_{3,4}=\pm i\omega_2$ are distinct pure imaginary numbers and the solution is bounded and is composed of two harmonic motions. The general solution is [3]:

$$\begin{aligned}\xi&=A_1\cos\omega_1 t+A_2\sin\omega_1 t+A_3\cos\omega_2 t+A_4\sin\omega_2 t\\ \eta&=B_1\cos\omega_1 t+B_2\sin\omega_1 t+B_3\cos\omega_2 t+B_4\sin\omega_2 t\end{aligned} \qquad (6)$$

Where

$$\omega_1=\left\{\mu(1-\mu)\left[\frac{27}{4}+\frac{33\in'}{2}+\frac{3(1-q_1)}{2}+\frac{3(1-q_2)}{2}+9\alpha_3+\frac{117}{4}(\alpha_1+\alpha_2)-\frac{M_d}{\left(r_c^2+T^2\right)^{\frac{3}{2}}}\left\{\frac{33}{2}-33r_c\right.\right.\right.$$

$$\left.\left.\left.-\frac{19}{4\left(r_c^2+T^2\right)}\right\}\right]+\frac{2M_d}{\left(r_c^2+T^2\right)^{5/2}}\right\}^{1/2} \qquad (7)$$

$$\omega_2=\left[1-\frac{3}{2}(1-2\mu)(\alpha_1-\alpha_2)-3\alpha_3-3\in'+8\in+\frac{M_d}{\left(r_c^2+T^2\right)^{3/2}}\left\{3+2r_c-\frac{2}{\left(r_c^2+T^2\right)}\right\}-\mu(1-\mu)\right. \qquad (8)$$

$$\left.\times\left\{\frac{27}{4}+\frac{117}{4}(\alpha_1+\alpha_2)+9\alpha_3+\frac{3}{2}(1-q_1)+\frac{3}{2}(1-q_2)+\frac{33}{2}\in'-\frac{M_d}{\left(r_c^2+T^2\right)^{3/2}}\left(\frac{33}{2}-33r_c-\frac{69}{12\left(r_c^2+T^2\right)}\right)\right\}\right]^{1/2}$$

ξ,η are small displacements applied at the triangular equilibrium points (4). The coefficients A_i and $B_i\,(i=1,2,3,4)$ are the long and short periodic terms respectively, while ω_1 and ω_2 are the frequency of the long and short periodic orbits, respectively. The value of the frequency of the long period orbit depends on the mass parameter, the centrifugal perturbation, the potential of cluster of material points, radiation pressures of the stars and oblateness of the bodies but does not depend on the Coriolis perturbation, while the frequency of the short period orbits is affected by all the perturbing forces. Below in Table 1, we estimate numerically the frequencies and periods in equations (7) and (8), for some chosen parametric values. We consider the stars to be a yellow supergiant eclipsing binary system, having the shape of an oblate spheroid and are mostly same in size. Hence, for all our numerical results, we take $\mu=0.48785$. In Table 2, we check the effects of cluster of material points on the frequencies and periods.

Table 1. Numerical evaluations of the angular frequencies and the period

q_1	q_2	α_1	α_2	α_3	$\in$	$\in'$	M_d	ω_1	ω_2	τ_1	τ_2
1	1	0	0	0	0	0	0	1.56079i	1.25058i	4.02565	5.02423
0.9988	1	0	0	0	0	0	0	1.56064i	1.25076i	4.02602	5.02351
1	0.9985	0	0	0	0	0	0	1.56061i	1.25080i	4.02611	5.02333
0.9988	0.9985	0	0	0	0	0	0	1.56046i	1.25098i	4.02648	5.02261
1	1	0.024	0	0	0	0	0	1.50355i	1.40156i	4.17890	4.48299
1	1	0	0.02	0	0	0	0	1.51324i	1.30743i	4.15214	4.80575
1	1	0	0	0.015	0	0	0	1.54995i	1.28167i	4.05381	4.90236
1	1	0	0	0	0.001	0	0	1.50355i	1.24737i	4.1789	5.03713
1	1	0	0	0	0	0.002	0	1.55814i	1.25626i	4.03248	5.00151
1	1	0	0	0	0	0	0.01	1.53476i	1.26607i	4.09391	4.96275
0.9988	1	0.024	0	0	0	0	0	1.50340i	1.31934i	4.17931	4.76237
0.9988	0.9985	0.024	0	0	0	0	0	1.50321i	1.31955i	4.17983	4.76160
0.9988	0.9985	0.024	0.02	0	0	0	0	1.45378i	1.37356i	4.32195	4.57439
0.9988	0.9985	0.024	0.02	0.015	0	0	0	1.44214i	1.40192i	4.35686	4.48183
0.9988	0.9985	0.024	0.02	0.015	0.001	0	0	1.44214i	1.24778i	4.35686	5.03550
0.9988	0.9985	0.024	0.02	0.015	0.001	0.002	0	1.43928i	1.40415i	4.36552	4.47473
0.9988	0.9985	0.024	0.02	0.015	0.001	0.002	0.01	1.41101i	1.41797i	4.45296	4.43113

In Table 1, the entry in row 1 corresponds to the classical case when the governing parameter is the mass ratio of the stars, while row 2 and row 3, are the cases of the RTBP with radiation effects of the first and second primary, respectively. As such, we have computed the numerical values of the frequencies and periods for the long and short period orbits by weighing the effects of each imposed parameter and then considering their combinations. Table 2 evaluates the effects of accumulation of material points around the stars on the angular frequencies and periods for $0 \le M_d \le 0.099$.

Table 2. Effect of accumulation of material points on angular frequencies and periods for $q_1 = 0.9988, q_2 = 0.9985, \alpha_1 = 0.024, \alpha_2 = 0.02, \alpha_3 = 0.015, \in = 0.001, \in' = 0.002$

M_d	ω_1	ω_2	$\tau_1(2\pi/\omega_1)$	$\tau_2(2\pi/\omega_2)$
0	1.43928i	1.40415i	4.36552	4.47473
0.01	1.41101i	1.41797i	4.45296	4.43113
0.02	1.38217i	1.43165i	4.54588	4.38877
0.03	1.35272i	1.44521i	4.64487	4.34761
0.04	1.32260i	1.45863i	4.75061	4.30758
0.05	1.29179i	1.47194i	4.86393	4.26864
0.06	1.26023i	1.48513i	4.98576	4.23074
0.07	1.22785i	1.49820i	5.11723	4.19383
0.08	1.19459i	1.51116i	5.25969	4.15787
0.09	1.16039i	1.52400i	5.41474	4.12281
0.099	1.12871i	1.53548i	5.56668	4.09201
0.0999	1.12550i	1.53662i	5.58259	4.08897

3.2 Elliptic Orbits and Their Orientation

Now, from equations (6), we select the initial conditions such that the coefficients of the short periodic terms of these equations are zero. In this case, we have an elliptic orbit and the periodic solution is

$$\begin{aligned}\xi &= A_1 \cos\omega_1 t + A_2 \sin\omega_1 t \\ \eta &= B_1 \cos\omega_1 t + B_2 \sin\omega_1 t\end{aligned} \tag{9}$$

Next, we expand the potential in equation (1) around the triangular points, to get

$$U = U^0 + \frac{1}{2}U^0_{xx}\xi^2 + U^0_{xy}\xi\eta + \frac{1}{2}U^0_{yy}\eta^2 + O\left(\xi^3, \eta^3\right) \tag{10}$$

Where

$$U^0_{xx} = \psi^{5/3}\left[\frac{3}{4} + \left(\frac{27}{8} - 3\mu\right)\alpha_1 + \left(\frac{3}{8} + 3\mu\right)\alpha_2 + \frac{5(2\psi r_c - 1)M_d}{4\psi\left(r_c^2 + T^2\right)^{3/2}}\right] + \psi\left[\frac{\left(\psi^{2/3} - 2\right)}{2}(1-q_1) + (1-q_2)\right.$$

$$\left. - \frac{\left(\psi^{2/3} - 4\right)\mu}{2}(1-q_1) + \frac{\left(\psi^{2/3} - 4\right)\mu}{2}(1-q_2)\right] - \frac{3(2\mu-1)^2 M_d}{4\left(r_c^2 + T^2\right)^{3/2}}\left[1 + \frac{1}{\psi^{2/3}\left(\mu - 1/2\right)}\left\{\frac{1}{3}(1-q_1) + \frac{1}{3}(1-q_2)\right.\right.$$

$$\left.\left. - \frac{1}{2}\psi^{2/3}(\alpha_1 - \alpha_2)\right\}\right]$$

$$U_{yy}^{0}=\frac{3M_d\left(4-\psi^{2/3}\right)}{4\psi^{2/3}\left(r_c^2+T^2\right)^{5/2}}+\psi\left[\frac{3\left(4-\psi^{2/3}\right)}{4}+\frac{3\left(12-\psi^{2/3}\right)\left(\alpha_1+\alpha_2\right)}{8}+3\alpha_3\psi^{2/3}+\frac{\left(1-q_1\right)\left(2-\psi^{2/3}\right)}{2}\right.$$
$$\left.-\left(1-q_2\right)+\frac{\left(20-13\psi^{2/3}\right)\left(2\psi r_c-1\right)M_d}{4\psi\left(r_c^2+T^2\right)^{3/2}}+\mu\left\{\frac{\left(4-\psi^{2/3}\right)}{2}\left(1-q_2\right)-\frac{\left(4-\psi^{2/3}\right)}{2}\left(1-q_1\right)\right\}\right] \quad (11)$$

$$U_{xy}^{0}=\psi^{4/3}\sqrt{4-\psi^{2/3}}\left[-\frac{3}{4}+\frac{\left(4-4\psi^{2/3}+\psi^{4/3}\right)\left(1-q_1\right)}{2\psi^{2/3}\left(4-\psi^{2/3}\right)}+\frac{\left(\psi^{2/3}-2\right)\left(1-q_2\right)}{\psi^{2/3}\left(4-\psi^{2/3}\right)}+\frac{3}{8}\frac{\left(5\psi^{2/3}-24\right)}{\left(4-\psi^{2/3}\right)}\alpha_1\right.$$
$$+\frac{3}{8}\frac{\left(\psi^{2/3}-8\right)}{\left(4-\psi^{2/3}\right)}\alpha_2-\frac{3}{2}\frac{\psi^{2/3}}{\left(4-\psi^{2/3}\right)}\alpha_3-\frac{\left(16-5\psi^{2/3}\right)}{4\psi\left(4-\psi^{2/3}\right)}\frac{\left(2\psi r_c-1\right)M_d}{\left(r_c^2+T^2\right)^{3/2}}+\mu\left\{\frac{3}{2}-\frac{\left(\psi^{2/3}-2\right)}{2\left(4-\psi^{2/3}\right)}\left(1-q_1\right)\right.$$
$$\left.-\frac{\left(\psi^{2/3}-2\right)}{2\left(4-\psi^{2/3}\right)}\left(1-q_2\right)-\frac{3\left(3\psi^{2/3}-16\right)}{4\left(4-\psi^{2/3}\right)}\left(\alpha_1+\alpha_2\right)+\frac{3\psi^{2/3}}{\left(4-\psi^{2/3}\right)}\alpha_3+\frac{\left(16-5\psi^{2/3}\right)\left(2\psi r_c-1\right)M_d}{2\psi\left(4-\psi^{2/3}\right)\left(r_c^2+T^2\right)^{3/2}}\right\}$$
$$\left.+\frac{3\left(2\mu-1\right)M_d}{4\psi^{5/3}\left(r_c^2+T^2\right)^{5/2}}\right]$$

$$U^{0}=\frac{n^2\psi}{2}\left[\left(1-\mu\right)r_1^2+\mu r_2^2\right]+\frac{q_1\left(1-\mu\right)}{r_1}+\frac{q_2\mu}{r_2}+\frac{\left(\alpha_1q_1+\alpha_3\right)\left(1-\mu\right)}{2r_1^3}+\frac{\left(\alpha_2q_2+\alpha_3\right)\mu}{2r_2^3}+\frac{M_d}{\left(r_c^2+T^2\right)^{1/2}} \quad (12)$$

Equation (12) is a symmetric form of the potential in (1) while equation (10) is in the quadratic form and shows that the orbits around the triangular points are ellipses.

Now equation (12) in its simplest form, is given as

$$U^{o}=\frac{3}{2}+\left(\frac{5}{4}-\frac{1}{2}\mu\right)\alpha_1+\left(\frac{3}{4}+\frac{1}{2}\mu\right)\alpha_2+\frac{1}{2}\alpha_3-\left(1-\mu\right)\left(1-q_1\right)-\mu\left(1-q_2\right)+\frac{1}{2}\in'+\frac{M_d}{\left(r_c^2+T^2\right)^{1/2}}$$
$$\times\left\{1+\frac{r_c}{\left(r_c^2+T^2\right)}\right\} \quad (13)$$

Using equation (13) in (10), gives

$$U=K\xi^2-M\xi\eta+N\eta^2+U^0 \quad (14)$$

Where

$$K=\frac{3}{8}+\left(\frac{27}{16}-\frac{3}{2}\mu\right)\alpha_1+\left(\frac{3}{16}+\frac{3}{2}\mu\right)\alpha_2-\left(\frac{1}{4}-\frac{3}{4}\mu\right)\left(1-q_1\right)+\left(\frac{1}{2}-\frac{3}{4}\mu\right)\left(1-q_2\right)+\frac{5}{8}\in+\frac{M_d}{\left(r_c^2+T^2\right)^{3/2}}$$
$$\times\left\{\frac{3}{8\left(r_c^2+T^2\right)}+\frac{5}{4}r_c-\frac{5}{8}-\frac{3\mu\left(1-\mu\right)}{2\left(r_c^2+T^2\right)}\right\}$$

$$M=\sqrt{3}\left[\frac{3}{4}-\frac{3\mu}{2}+\left(\frac{19}{8}-\frac{13\mu}{4}\right)\alpha_1+\left(\frac{7}{8}-\frac{13\mu}{4}\right)\alpha_2+\left(\frac{1}{2}+\mu\right)\alpha_3-\left(\frac{1}{6}+\frac{\mu}{6}\right)(1-q_1)+\left(\frac{1}{3}+\frac{\mu}{6}\right)(1-q_2)\right.$$

$$\left.+\left(\frac{11}{12}-\frac{11}{6}\mu\right)\in'-\frac{M_d}{\left(r_c^2+T^2\right)^{3/2}}\left\{\left(\frac{11}{12}-\frac{11\mu}{6}\right)-\left(\frac{11}{6}-\frac{11\mu}{3}\right)r_c-\frac{3}{\left(r_c^2+T^2\right)}+\frac{3\mu}{2\left(r_c^2+T^2\right)}\right\}\right]$$

$$N=\frac{9}{8}+\frac{33}{16}(\alpha_1+\alpha_2)+\frac{3}{2}\alpha_3+\frac{7}{8}\in'+\frac{1}{4}(1-3\mu)(1-q_1)-\frac{1}{4}(2-3\mu)(1-q_2)-\left\{\frac{7}{2}-7r_c-\frac{9}{2\left(r_c^2+T^2\right)}\right\}$$

$$\times\frac{M_d}{4\left(r_c^2+T^2\right)^{3/2}}$$

Introducing the variables, $\bar{\xi}$ and $\bar{\eta}$ by the transformation:

$$\begin{aligned}\xi&=\bar{\xi}\cos\alpha-\bar{\eta}\sin\alpha\\ \eta&=\bar{\xi}\sin\alpha+\bar{\eta}\cos\alpha\end{aligned}\tag{15}$$

This is equivalent to the rotation of the coordinate system $\xi\ \eta$ through angle α as illustrated in Fig. 1 below.

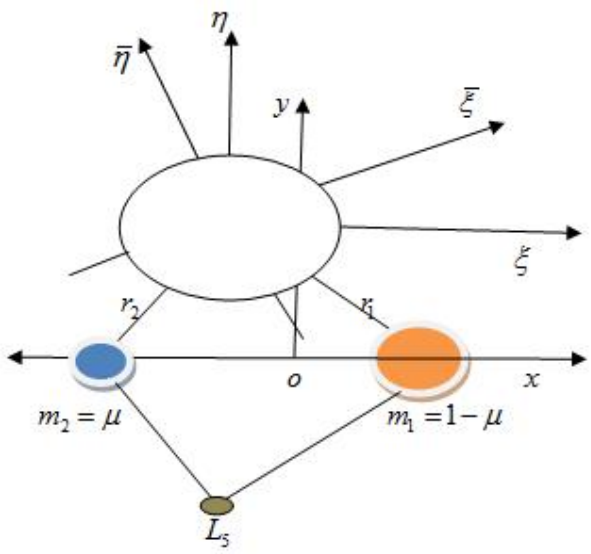

Fig. 1. Orientation of the principal axes for the periodic orbits

If we select α such that the terms containing $\bar{\xi}\bar{\eta}$ in the force function U is zero, we get the new force function in its simplified quadratic form:

$$\bar{U}=B_1\bar{\xi}^2+B_2\bar{\eta}^2+U^0\tag{16}$$

Where

$$B_1=\frac{3}{8}+\frac{3}{4}\sin^2\alpha-\frac{3\sqrt{3}}{8}(1-2\mu)\sin 2\alpha+\left[\frac{27}{16}-\frac{3}{2}\mu+\left(\frac{3}{8}+\frac{3}{2}\mu\right)\sin^2\alpha-\frac{\sqrt{3}}{2}\left(\frac{19}{8}-\frac{13}{4}\mu\right)\sin 2\alpha\right]\alpha_1$$
$$+\left[\frac{3}{16}+\frac{3\mu}{2}+\left(\frac{15}{8}-\frac{3\mu}{2}\right)\sin^2\alpha-\frac{\sqrt{3}}{2}\left(\frac{7}{8}-\frac{13\mu}{4}\right)\sin 2\alpha\right]\alpha_2+\left[\frac{3}{2}\sin^2\alpha-\frac{\sqrt{3}}{2}\left(\frac{1}{2}+\mu\right)\sin 2\alpha\right]\alpha_3$$
$$+\left[\left(-\frac{1}{4}+\frac{3\mu}{4}\right)\cos 2\alpha+\frac{\sqrt{3}}{2}\left(\frac{1}{6}+\frac{\mu}{6}\right)\sin 2\alpha\right](1-q_1)+\left[\left(\frac{1}{2}-\frac{3\mu}{4}\right)\cos 2\alpha+\frac{\sqrt{3}}{2}\left(-\frac{1}{3}+\frac{\mu}{6}\right)\sin 2\alpha\right](1-q_2)$$
$$+\left[\frac{5}{8}+\frac{1}{4}\sin^2\alpha-\frac{11\sqrt{3}(1-2\mu)}{24}\sin 2\alpha\right]\in'+\left[\left\{\frac{5}{4}r_c-\frac{5}{8}+\frac{3}{8\left(r_c^2+T^2\right)}-\frac{3\mu(1-\mu)}{2\left(r_c^2+T^2\right)}\right\}+\left\{\frac{r_c}{2}-\frac{1}{4}+\frac{3}{4\left(r_c^2+T^2\right)}\right.\right.$$
$$\left.\left.+\frac{3\mu(1-\mu)}{2\left(r_c^2+T^2\right)}\right\}\sin^2\alpha+\frac{\sqrt{3}}{2\left(r_c^2+T^2\right)^{3/2}}\left\{\left(\frac{11}{12}-\frac{11\mu}{6}\right)-\left(\frac{11}{6}-\frac{11\mu}{3}\right)r_c-\frac{3}{\left(r_c^2+T^2\right)}+\frac{3\mu}{2\left(r_c^2+T^2\right)}\right\}\sin 2\alpha\right]M_d$$

$$B_2=\frac{3}{8}+\frac{3}{4}\cos^2\alpha+\frac{3\sqrt{3}}{8}(1-2\mu)\sin 2\alpha+\left[\frac{27}{16}-\frac{3}{2}\mu+\left(\frac{3}{8}+\frac{3}{4}\mu\right)\cos^2\alpha+\frac{\sqrt{3}}{2}\left(\frac{19}{8}-\frac{13}{4}\mu\right)\sin 2\alpha\right]\alpha_1$$
$$+\left[\frac{3}{16}+\frac{3}{2}\mu+\left(\frac{15}{8}-\frac{3}{2}\mu\right)\cos^2\alpha+\frac{\sqrt{3}}{2}\left(\frac{7}{8}-\frac{13}{4}\mu\right)\sin 2\alpha\right]\alpha_2+\left[\frac{3}{2}\cos^2\alpha+\frac{\sqrt{3}}{2}\left(\frac{1}{2}+\mu\right)\sin 2\alpha\right]\alpha_3$$
$$+\left[\left(\frac{1}{4}-\frac{3\mu}{4}\right)\cos 2\alpha-\frac{\sqrt{3}}{2}\left(\frac{1}{6}+\frac{\mu}{6}\right)\sin 2\alpha\right](1-q_1)-\left[\left(\frac{1}{2}-\frac{3\mu}{4}\right)\cos 2\alpha-\frac{\sqrt{3}}{2}\left(\frac{\mu}{6}-\frac{1}{3}\right)\sin 2\alpha\right](1-q_2)$$
$$+\left[\frac{5}{8}+\frac{1}{4}\cos^2\alpha+\frac{11(1-2\mu)\sqrt{3}}{24}\sin 2\alpha\right]\in'+\frac{M_d}{\left(r_c^2+T^2\right)^{3/2}}\left[\left\{\frac{5}{4}r_c-\frac{5}{8}+\frac{3}{8\left(r_c^2+T^2\right)}-\frac{3\mu(1-\mu)}{2\left(r_c^2+T^2\right)}\right\}\right.$$
$$+\left\{\frac{1}{2}r_c-\frac{1}{4}+\frac{3}{4\left(r_c^2+T^2\right)}+\frac{3\mu(1-\mu)}{2\left(r_c^2+T^2\right)}\right\}\cos^2\alpha+\frac{\sqrt{3}}{2}\left\{\left(\frac{11}{12}-\frac{11\mu}{6}\right)-\left(\frac{11}{6}-\frac{11\mu}{3}\right)r_c-\frac{3}{\left(r_c^2+T^2\right)}\right.$$
$$\left.\left.+\frac{3\mu}{2\left(r_c^2+T^2\right)}\right\}\sin 2\alpha\right]$$

Now, to get the orientation of the orbits, we set the term having coefficient $\xi\eta$ to zero, in equation (14). We do this by substituting terms in ξ^2 for those in η^2, and the principal axes of the curve of zero velocity are oriented such that

$$\alpha=\frac{1}{2}\arctan\left\{\frac{4\sqrt{3}}{3}\left[\frac{3}{4}-\frac{3}{2}\mu+\left(\frac{2}{3}-\frac{4\mu}{3}\right)\in'+\left(2-4\mu+3\mu^2\right)\alpha_1-\left(1-2\mu+3\mu^2\right)\alpha_2-(1-4\mu)\alpha_3\right.\right.$$
$$+\left(\frac{2}{3}-\frac{7\mu}{3}+3\mu^2\right)(1-q_1)+\left(\frac{4}{3}-\frac{11\mu}{3}+3\mu^2\right)(1-q_2)-\left\{1-\frac{16r_c}{9}+\frac{4\mu(2r_c-1)-18-54\mu^2+36\mu^3}{9\left(r_c^2+T^2\right)}\right\}$$
$$\left.\left.\times\frac{3M_d}{4\left(r_c^2+T^2\right)^{3/2}}\right]\right\} \qquad (17)$$

The orientation described by equation (17) is determined by the perturbed forces of radiation pressure of the stars, oblateness of three bodies, potential from the circular cluster of materials and small change in the centrifugal perturbation. In Table 3, we compute numerically the angle α of rotation of the principal axis (17), by an exploration which allows us to estimate the effect of each perturbing force on the orientation of the principal axis. We have numbered the rows in Table 3 from 1 to 17. Row 1 corresponds to the case of the classical RTBP when the determining parameter is the mass ratio. Row 2 and 3 consider the effect of radiation pressure of the primary and secondary star, respectively; and onto row 17, which is the generalized case.

The angles, by which the axis deviate based on the effects of the perturbing forces, are the entries on the last column of Table 3. We observe that the angle α on row1 and that on row 8 coincide because equation (17) is not affected by the Coriolis perturbation. Same goes for row14 and 15. From our numerical evidence, we notice that the accumulation of material points around the stars has a major influence on the rotation of the principal axis than any other perturbing force as seen in row 10, while interestingly; oblateness of the secondary star reduces the angle of rotation immensely (row 6). However, under the combined effects of radiation, oblateness of the bodies, centrifugal perturbation and the presence of a circular cluster of material points, the angle of rotation of the principal axis increases, as seen in row 17. These facts are not directly observable from the analytic solution given in equation (17).

In Tables 4 and 5, we compute numerical the periodic terms A_i , $B_i\left(i=1,2\right)$, the angular frequency ω_1 and period τ under effect of oblateness of the infinitesimal mass and accumulation of material points, respectively.

Table 4 gives the numerical evaluations of effect of oblateness of the infinitesimal mass on the periodic terms, frequency and period of the orbits. Evidently, an increase in oblateness of the infinitesimal body leads to an increase and a decrease in the angular frequency and period, respectively. The converse is the case in Table 5, where it is seen that an increase in the mass of the circular cluster of materials results in a decrease and an increase in the angular frequency and period of the orbits, respectively. Below in Fig. 2 and Fig. 3, we have drawn the orbits of the infinitesimal mass on the $\xi\eta-$plane under effects of oblateness of the infinitesimal mass by substituting the numerical estimations of the periodic terms, angular frequency and the period given in Table 4, in equation (9) and using the software *Mathematica* [18] to plot the orbits. Similarly, using Table 5, we have also drawn the orbits as a function of increasing mass of the clusters around the stars in Fig. 4.

Table 3. Effect of perturbed forces on angle of rotation of the principal axis

S/N	q_1	q_2	α_1	α_2	α_3	$\in$	$\in'$	M_d	$\tan 2\alpha$	α
1	1	1	0	0	0	0	0	0	0.042088	1.2050
2	0.9988	1	0	0	0	0	0	0	0.042760	1.2242
3	1	0.9985	0	0	0	0	0	0	0.042984	1.2306
4	0.9988	0.9985	0	0	0	0	0	0	0.043656	1.2498
5	1	1	0.024	0	0	0	0	0	0.084356	2.4109
6	1	1	0	0.02	0	0	0	0	0.007988	0.2288
7	1	1	0	0	0.015	0	0	0	0.075046	2.1458
8	1	1	0	0	0	0.001	0	0	0.042088	1.2050
9	1	1	0	0	0	0	0.002	0	0.042014	1.2029
10	1	1	0	0	0	0	0	0.01	0.156119	4.4366
11	0.9988	1	0.024	0	0	0	0	0	0.085027	2.4300
12	0.9988	0.9985	0.024	0	0	0	0	0	0.085923	2.4554
13	0.9988	0.9985	0.024	0.02	0	0	0	0	0.051823	1.4832
14	0.9988	0.9985	0.024	0.02	0.015	0	0	0	0.084780	2.4229
15	0.9988	0.9985	0.024	0.02	0.015	0.001	0	0	0.084780	2.4229
16	0.9988	0.9985	0.024	0.02	0.015	0.001	0.002	0	0.084705	2.4208
17	0.9988	0.9985	0.024	0.02	0.015	0.001	0.002	0.01	0.198736	5.6201

Table 4. Effects of oblateness of the infinitesimal mass on the periodic terms for $q_1 = 0.9988$, $q_2 = 0.9985, \alpha_1 = 0.024, \alpha_2 = 0.02, \in = 0.001, \in' = 0.002, M_d = 0.01$

α_3	A_1	A_2	B_1	B_2	ω_1	$\tau(2\pi/\omega_1)$
0	-0.0122499	0.766013	0.856043	-0.152587	1.36267	3.38374
0.004	-0.0142499	0.772941	0.845676	-0.158754	1.479	2.8724
0.008	-0.0142499	0.77448	0.847987	-0.15942	1.48203	2.86064
0.01	-0.0142499	0.77525	0.849143	-0.159754	1.48355	2.8548
0.015	-0.0142499	0.777175	0.852032	-0.160587	1.48734	2.84029
0.02	-0.0142499	0.779099	0.854922	-0.16142	1.49111	2.82592
0.024	-0.0142499	0.780639	0.857233	-0.162087	1.49412	2.81454

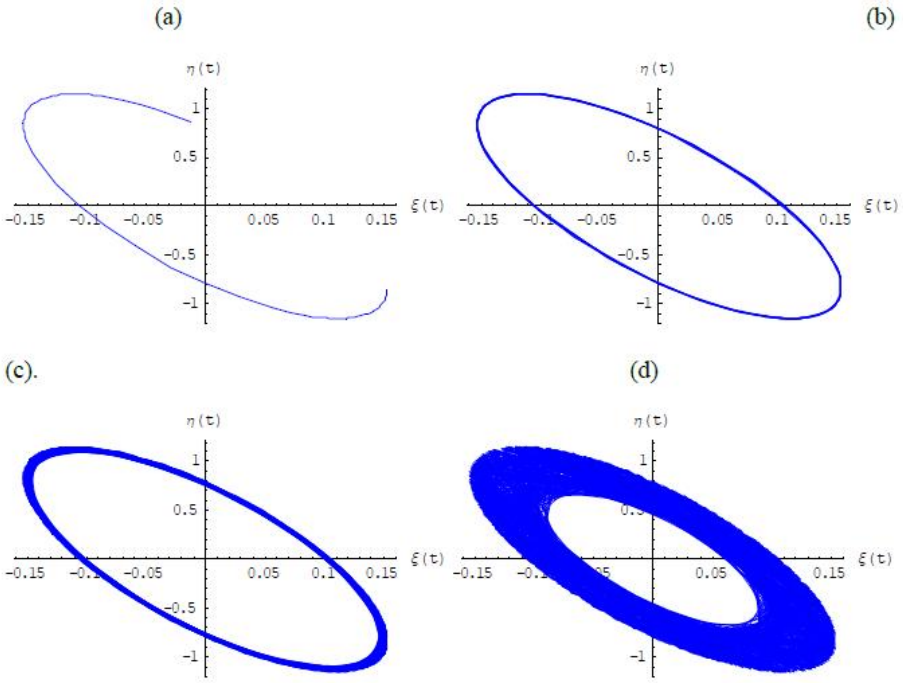

Fig. 2. Elliptic orbits when $\alpha_3 = 0, q_1 = 0.9988, q_2 = 0.9985, \alpha_1 = 0.024, \alpha_2 = 0.02, \in = 0.001, \in' = 0.002, M_d = 0.01$ and (a), $t = \tau = 3.38374$ (b) $t = 10\tau$ (c) $t = 100\tau$ (d) $t = 300\tau$

Table 5. Numerical evaluations of periodic terms under effects of accumulation of materials for $q_1 = 0.9988, q_2 = 0.9985, \alpha_1 = 0.024, \alpha_2 = 0.02, \alpha_3 = 0.015, \in = 0.001, \in' = 0.002$

M_d	A_1	A_2	B_1	B_2	ω_1	τ
0	-0.0142499	0.785141	0.860726	-0.149292	1.43928i	4.36552
0.01	-0.0142499	0.777573	0.856379	-0.153342	1.41101i	4.45296
0.02	-0.0142499	0.770006	0.852032	-0.157392	1.38217i	4.54588
0.03	-0.0142499	0.762438	0.847685	-0.161442	1.35272i	4.64487
0.04	-0.0142499	0.754871	0.843339	-0.165492	1.32260i	4.75061
0.05	-0.0142499	0.747303	0.838992	-0.169542	1.29179i	4.86393
0.06	-0.0142499	0.739736	0.834645	-0.173592	1.26023i	4.98576
0.07	-0.0142499	0.732168	0.830298	-0.177642	1.22785i	5.11723
0.08	-0.0142499	0.7246	0.825951	-0.181693	1.19459i	5.25969
0.09	-0.0142499	0.717033	0.821604	-0.185743	1.16039i	5.41474
0.099	-0.0142499	0.710222	0.817692	-0.189388	1.12871i	5.56668

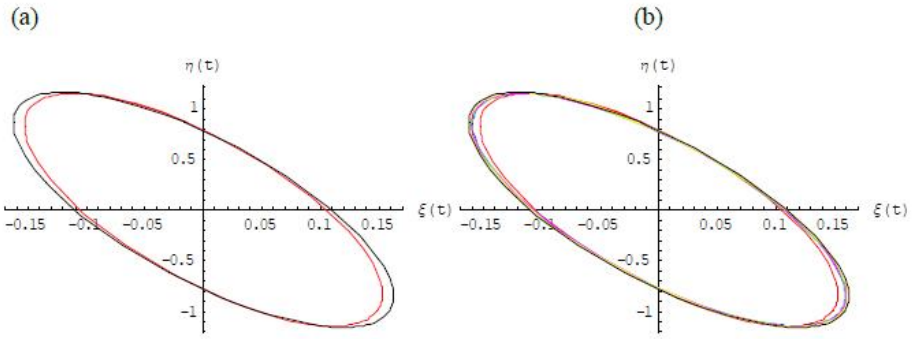

Fig. 3. Elliptic orbits under effects of oblateness of the infinitesimal mass when $\alpha_1 = 0.024$, $\alpha_2 = 0.02$, $q_1 = 0.9988$, $q_2 = 0.9985$, $\in = 0.001$, $\in' = 0.002$, $M_d = 0.01$ **and (a)** $\alpha_3 = 0$ **(red orbit);** $\alpha_3 = 0.024$ **(black orbit) (b)** $0 \le \alpha_3 \le 0.024$

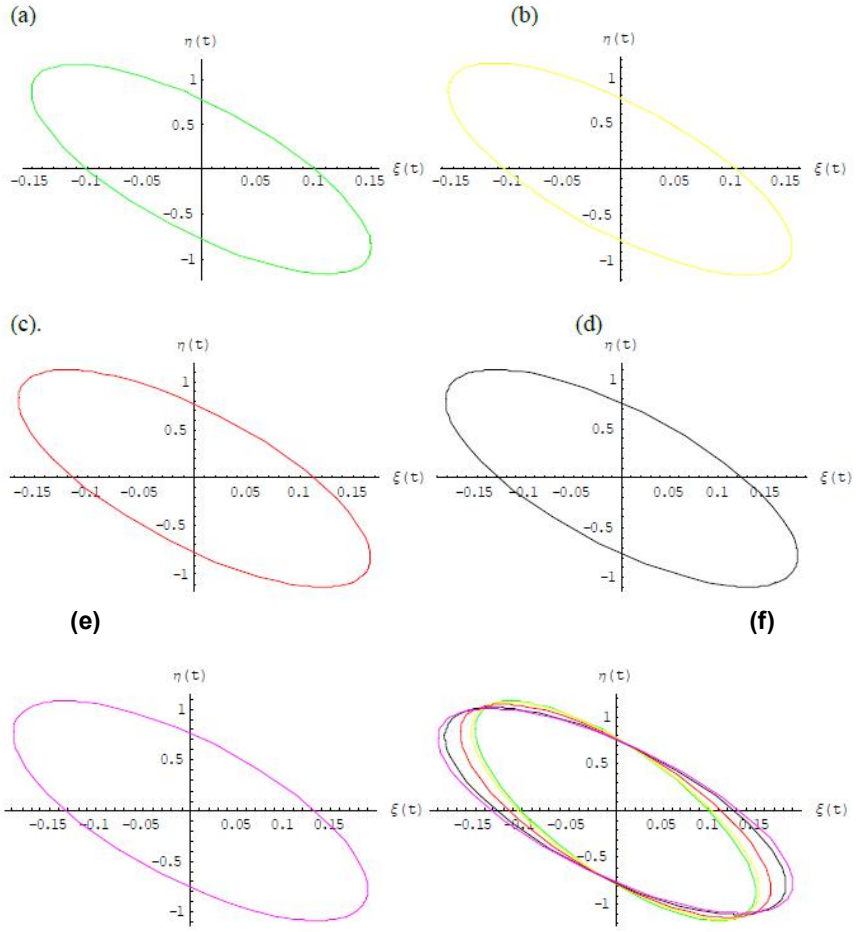

Fig. 4. Elliptic orbits with increasing mass of cluster of material points around the primaries for $\alpha_1 = 0.024$, $\alpha_2 = 0.02$, $\alpha_3 = 0.015$, $q_1 = 0.9988$, $q_2 = 0.9985$, $\in = 0.001$ **and** $\in' = 0.002$, **when (a)** $M_d = 0$ **(b)** $M_d = 0.01$ **(c)** $M_d = 0.04$ **(d)** $M_d = 0.08$ **(e)** $M_d = 0.099$ **(f) The elliptic orbits when plane (a), (b), (c), (d) and (e) are combined;** $M_d = 0$ **(green orbit),** $M_d = 0.01$ **(yellow orbit),** $M_d = 0.04$ **(red orbit),** $M_d = 0.08$ **(black orbit),** $M_d = 0.099$ **(purple colored orbit)**

The paths drawn in panel (a), (b), (c), (d) in Fig. 2 are the orbits of the infinitesimal mass plotted at different time when the third body is a sphere and the time is increased from $t = 3.38374$ (panel a) to $t = 1015.122$ (panel d). From these figures, it can be seen that the orbits have regular elliptic shape and the paths are retained for long time $t > 0$, even when $t = 300T$, the shape of the orbit remains same as for $t = 10T$. In Fig. 3, the effects of variations in oblateness of the infinitesimal mass are shown. The red orbit in panel (a) is when the infinitesimal mass is a sphere and is drawn using the entries on the first row in Table 4 while the black orbit is drawn using the entries on the last row in Table 4 when $\alpha_3 = 0.024$. Each orbit in panel (b) has been drawn from the corresponding entries in the first to the last row (i.e., $0 \le \alpha_3 \le 0.024$) in Table 4. The effects of variations in mass of accumulated material points combined with other perturbing forces, on the elliptic orbits of the infinitesimal mass have been shown in Fig. 4.

In Table 6, we have computed values for the periodic terms by trying to estimate the effects of each perturbing force on them and next, we proceed to plot the orbits in Fig. 5 using our numerical evaluations recorded in Table 6. However, we only plot orbits which appear distinct from one another and also we combine some plots to show the effects of the perturbing forces on the elliptic orbits of the infinitesimal mass around triangular equilibrium points.

The figures above have been drawn to show the influence of each perturbing force on the elliptic orbits of the infinitesimal mass using Table 6. The panel (a) corresponds to the orbit around the triangular points of the classical RTBP and has been plotted using the numerical values in row 1 of Table 6. The figure in panel (b) is the orbit around triangular equilibrium points of the RTBP with an oblate primary star and has been plotted by using the values on row 5 in Table 6. The figure in Panel (c) which has been drawn using the values on row 6 is the elliptic orbit under effects of oblateness of the secondary star, while panel (d) is the orbit under combined effects of oblateness, radiation, perturbations and cluster of points around the stars. The combination of the orbits in panel (e) helps us to see how the orbit looks like in the case of the classical RTBP (red orbit) and what it turns out like (blue orbit) under the combined effects of the perturbing forces we studied in this paper. Panel (f) explains orbits of three cases. The red orbit is for the classical model of the RTBP, the green type shows the effect of accumulated materials around the stars while the blue orbit is for our generalized model. The last figure in panel (g) is the combination of orbits of all the cases in Table 6.

4. ECCENTRICITY AND SEMI-AXES OF THE ELLIPTIC ORBITS

The equation (3) has the associated characteristic equation of the form

$$\sigma^2 - \left[3 + 3\in' + \left(\frac{15}{2} - 3\mu\right)\alpha_1 + \left(\frac{9}{2} + 3\mu\right)\alpha_2 + 3\alpha_3 + \frac{3M_d}{\left(r_c^2 + T^2\right)^{3/2}}\left\{2r_c - 1 + \frac{4 + \mu - \mu^2}{4\left(r_c^2 + T^2\right)}\right\}\right]\sigma + \frac{27}{4}\mu(1-\mu)$$

$$+\mu(1-\mu)\left[\frac{117(\alpha_1 + \alpha_2)}{4} + 9\alpha_3 + \frac{3(1-q_1)}{2} + \frac{3(1-q_2)}{2} + \frac{33\in'}{4} - \frac{3M_d}{2\left(r_c^2 + T^2\right)^{3/2}}\left\{11 - 2r_c - \frac{9}{2\left(r_c^2 + T^2\right)}\right\}\right] = 0$$

The roots are

$$\sigma_1 = 3 - \frac{9}{4}\mu(1-\mu) + \left(\frac{15}{2} - \frac{51\mu}{4} + \frac{39\mu^2}{4}\right)\alpha_1 + \left(\frac{9}{2} - \frac{27\mu}{2} + \frac{39}{4}\mu^2\right)\alpha_2 + \left(3 - 3\mu + 3\mu^2\right)\alpha_3$$

$$+\frac{3\mu(1-\mu)}{2\left(r_c^2 + T^2\right)^{3/2}}\left\{\frac{11}{3} - 22r_c - \frac{3}{2\left(r_c^2 + T^2\right)}\right\}M_d + \left(3 - \frac{11\mu}{2} + \frac{11}{2}\mu^2\right)\in' - \frac{1}{2}\mu(1-\mu)(1-q_1) \qquad (18)$$

$$-\frac{1}{2}\mu(1-\mu)(1-q_2)$$

Table 6. Numerical estimations of effect of the perturbing forces on the periodic terms

q_1	q_2	α_1	α_2	α_3	$\in$	$\in'$	M_d	A_1	A_2	B_1	B_2
1	1	0	0	0	0	0	0	-0.0122	0.7815	0.8660	-0.1443
0.9988	1	0	0	0	0	0	0	-0.0117	0.7817	0.8657	-0.1443
1	0.9985	0	0	0	0	0	0	-0.0126	0.7817	0.8657	-0.1443
0.9988	0.9985	0	0	0	0	0	0	-0.0122	0.7819	0.8655	-0.1443
1	1	0.024	0	0	0	0	0	-0.0242	0.7894	0.8590	-0.1473
1	1	0	0.02	0	0	0	0	-0.0022	0.7792	0.8603	-0.1468
1	1	0	0	0.015	0	0	0	-0.0122	0.7874	0.8746	-0.1468
1	1	0	0	0	0.001	0	0	-0.0142	0.7931	0.8619	-0.1523
1	1	0	0	0	0	0.002	0	-0.0122	0.7804	0.8653	-0.1445
1	1	0	0	0	0	0	0.01	-0.0122	0.7740	0.8616	-0.1484
0.9988	1	0.024	0	0	0	0	0	-0.0237	0.7895	0.8588	-0.1473
0.9988	0.9985	0.024	0	0	0	0	0	-0.0242	0.7897	0.8585	-0.1472
0.9988	0.9985	0.024	0.02	0	0	0	0	-0.0142	0.7873	0.8528	-0.1497
0.9988	0.9985	0.024	0.02	0.015	0	0	0	-0.0142	0.7930	0.8614	-0.1522
0.9988	0.9985	0.024	0.02	0.015	0.001	0	0	-0.0142	0.7934	0.8614	-0.1522
0.9988	0.9985	0.024	0.02	0.015	0.001	0.002	0	-0.0142	0.7923	0.8607	-0.1524
0.9988	0.9985	0.024	0.02	0.015	0.001	0.002	0.01	-0.0142	0.7847	0.8563	-0.1565

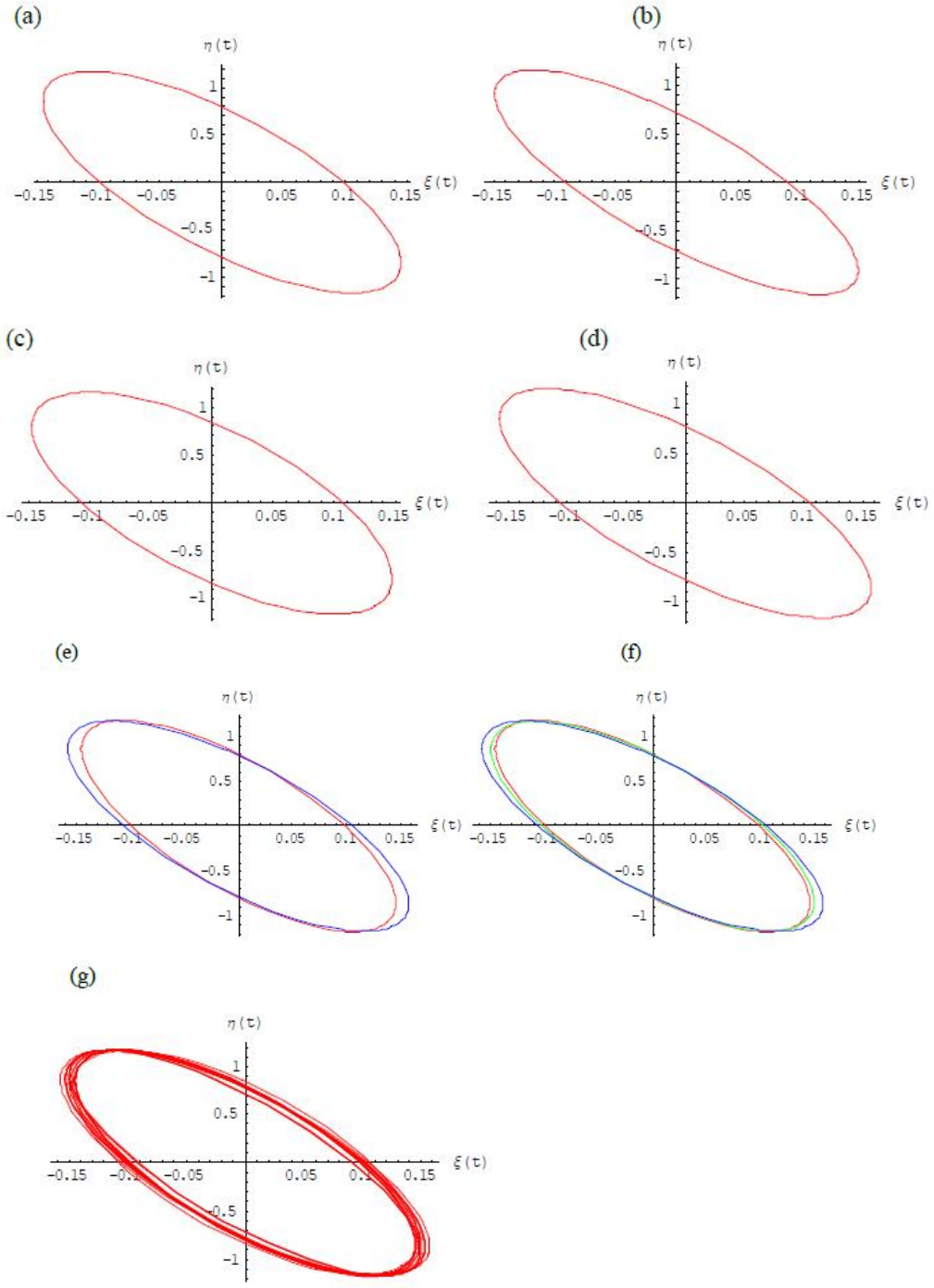

Fig. 5. Elliptic orbits of the infinitesimal mass around triangular points in the case of (a) model of the classical RTBP (b) oblate primary star (c) oblate secondary star (d) generalized model (e) classical case (red orbit) and generalized model (blue orbit) (f) classical model (red orbit), presence of circular clusters (green) and generalized problem (blue orbit) (g) all perturbing forces from row 1 to row17

$$\sigma_2 = \mu(1-\mu)\left[\frac{9}{4}+\frac{39}{4}(\alpha_1+\alpha_2)+3\alpha_3+\frac{11}{2}\in'+\frac{1}{2}(1-q_1)+\frac{1}{2}(1-q_2)-\frac{11M_d}{2\left(r_c^2+T^2\right)^{3/2}}-\frac{21M_d}{4\left(r_c^2+T^2\right)^{5/2}}\right]$$

$$-\frac{3M_d}{\left(r_c^2+T^2\right)^{3/2}}\left\{1-2r_c-\frac{1}{\left(r_c^2+T^2\right)}\right\}$$

In order to get the eccentricity of the ellipse, we use the relations given by Szebehely (1967):

$$e = \left(1-\delta^2\right)^{1/2} \tag{19}$$

Where

$$\delta_1 = \frac{2\omega_1}{\omega_1^2+\sigma_1}, \tag{20}$$

Using equation (7) and the first equation of (18) in equation (20), and retaining only linear terms in the parameters representing the introduced perturbed forces, we get

$$\delta^2 = 3\mu-12\mu^2-2\left(\mu+35\mu^2\right)\alpha_1+4\left(\mu-22\mu^2\right)\alpha_2-2\left(\mu+11\mu^2\right)\alpha_3+\frac{2}{3}\mu(1-7\mu)(1-q_1)$$

$$+\frac{2}{3}\mu(1-7\mu)(1-q_2)+\frac{4}{3}\mu(1-34\mu)\in'+\frac{M_d}{\left(r_c^2+T^2\right)^{3/2}}\left[\frac{8}{9\left(r_c^2+T^2\right)}-\left\{\frac{22}{3}-\frac{11r_c}{3}+\frac{41}{9\left(r_c^2+T^2\right)}\right\}\mu\right.$$

$$\left.+\left\{\frac{154}{3}-\frac{143r_c}{3}-\frac{61\mu(1-\mu)}{9\left(r_c^2+T^2\right)}\right\}\mu^2\right] \tag{21}$$

Substituting (21) in equation (19), the eccentricity of the orbit is obtained:

$$e = 1+\frac{3\mu}{2}(1-4\mu)+\left(\mu+35\mu^2\right)\alpha_1-2\left(\mu-22\mu^2\right)\alpha_2+\left(\mu+11\mu^2\right)\alpha_3-\frac{2}{3}\mu(1-34\mu)\in'$$

$$+\frac{M_d}{\left(r_c^2+T^2\right)^{3/2}}\left[\frac{4}{9\left(r_c^2+T^2\right)}-\left\{\frac{11}{3}-\frac{11r_c}{6}+\frac{41}{18\left(r_c^2+T^2\right)}\right\}\mu+\left\{\frac{77}{3}-\frac{143r_c}{6}-\frac{61}{18\left(r_c^2+T^2\right)}\right\}\mu^2\right] \tag{22}$$

$$-\frac{1}{3}\mu(1-7\mu)(1-q_1)-\frac{1}{3}\mu(1-7\mu)(1-q_2)$$

This equation gives the value by which the orbit departs from been circular. Clearly, the eccentricity of elliptical orbits depends on the mass ratio, small change in the centrifugal force, oblateness of the three bodies, radiation pressure of the stars and cluster of materials.

Now, we proceed to find the lengths of the semi-major axis a and semi-minor axis b of the elliptical orbits. from the relations

$$a=\frac{\sqrt{\xi_0^2\delta^2+\eta_0^2}}{\delta},\qquad b=\sqrt{\xi_0^2\delta^2+\eta_0^2} \tag{23}$$

where δ is given in equation (21) while ξ_0 and η_0 are given in (4) as initial conditions (Szebehely 1967), and so we consider the origin of coordinates system to be the triangular points L_4. Therefore, the lengths of the semi-major and semi-minor axes are

$$\begin{aligned}a=\frac{\sqrt{5}}{2}\Bigg[&1+\frac{2}{5}\mu(1-\mu)+\frac{1}{10\mu}+\left(\frac{34}{15}-\frac{2}{5}\mu\right)\alpha_1+\left(\frac{37}{15}+\frac{2}{5}\mu-\frac{1}{5\mu}\right)\alpha_2+\left(\frac{19}{15}+\frac{1}{5\mu}\right)\alpha_3\\&+\left(\frac{7}{45}-\frac{4}{15}\mu+\frac{1}{5\mu}\right)(1-q_1)+\left(\frac{1}{9}-\frac{4}{15}\mu-\frac{1}{15\mu}\right)(1-q_2)-\left(\frac{2}{9}+\frac{2}{15\mu}\right)\in'+\frac{M_d}{\left(r_c^2+T^2\right)^{3/2}}\\&\times\left\{\left(\frac{61}{45}-\frac{1}{3\mu}\right)-\left(\frac{79}{90}-\frac{3}{10\mu}\right)r_c-\frac{1}{\left(r_c^2+T^2\right)}\left(\frac{61}{135}+\frac{41}{270\mu}-\frac{4}{135\mu^2}\right)\right\}\Bigg]\end{aligned} \tag{24}$$

$$\begin{aligned}b=\frac{\sqrt{3}}{2}\Bigg[&1+\frac{1}{2}\mu+\left(\frac{1}{3}-\frac{2}{3}\mu+\frac{49}{3}\mu^2\right)\alpha_1-\left(\frac{1}{3}+\frac{1}{3}\mu+\frac{34}{3}\mu^2\right)\alpha_2+\left(\frac{2}{3}-\frac{1}{3}\mu-\frac{7}{3}\mu^2\right)\alpha_3\\&-\left(\frac{2}{9}+\frac{5}{9}\mu-\frac{25}{9}\mu^2\right)(1-q_1)-\left(\frac{2}{9}-\frac{7}{9}\mu+\frac{47}{9}\mu^2\right)(1-q_2)-\left(\frac{4}{9}-\frac{2}{9}\mu+\frac{76}{9}\mu^2\right)\in'-\frac{M_d}{\left(r_c^2+T^2\right)^{3/2}}\\&\times\left\{\frac{4(1-2r_c)}{9}+\frac{4}{27\left(r_c^2+T^2\right)}-\left(\frac{11}{19}-\frac{11r_c}{18}+\frac{1}{6\left(r_c^2+T^2\right)}\right)\mu+\left(\frac{121}{9}-\frac{181r_c}{18}+\frac{45}{18\left(r_c^2+T^2\right)}\right)\mu^2\right\}\Bigg]\end{aligned} \tag{25}$$

The eccentricity of the ellipse is represented in equation (22) and gives the value by which the orbit departs from been circular. Clearly, the eccentricity of elliptical orbits depends on the mass ratio, small change in the centrifugal force, oblateness of the three bodies and radiation pressure of the stars. The lengths of the semi-major axis, a and the semi-minor axis, b of the elliptical orbits have been calculated and given in equations (24) and (25), respectively. Table 7 below gives the effect of the perturbed forces on the eccentricity, semi-major and semi-minor axes of the elliptic orbits, using equations (22), (24) and (25), respectively. From the Table 7, the lengths of the semi-major and minor axes in the case of the classical RTBP (row 1) are 1.4589 and 1.0772, respectively. Using this as a metric, we can estimate the effects of each perturbing force on the lengths of the semi-axes. Row 2 is the case when the primary star is a radiating source. Due to the radiation pressure, an increase is noticed in the lengths of both semi-axes. When the secondary star is a radiating body (row 3) a decrease in the lengths of both semi-axes is observed. In the case when both stars are radiating bodies (row 4); the length of the semi-major axis increases while the length of the minor-axis reduces. The increase and decrease in the lengths of the major and minor axes are aided by the radiation pressure of the primary and secondary star, respectively. Row 5, 6 and 7 show the numerical values of effects of oblateness of the primary star, secondary star and the infinitesimal mass, respectively. Here, oblateness of the primary star yields an increase in the lengths of the semi-axes while oblateness of the secondary star and the infinitesimal mass produce an increase in the length of the major axes and a reduction in the length of the semi-minor axes.

The small perturbation in the Coriolis force does not affect the lengths of the semi-axes since both lengths (row 8) coincide with those (row 1) of the classical RTBP. This fact is also clearly noticed in equations (24) and (25). The centrifugal

perturbation however affects the lengths of the semi-axes as its presence yields a decrease in the lengths of both semi-axes. An increase in the amount of the accumulated materials around the stars leads to a decrease in the lengths of the semi-axes (row 10). This means that an increase in the accumulated materials brings the infinitesimal mass closer to the triangular equilibrium points. When the stars are both radiating and the bodies in the configuration have the shape of an oblate spheroid, the combined actions of these perturbing forces increases the length of the semi-major axes of the elliptic orbits around the triangular points (row 14).

Below in Fig. 6, we plot some graphs to show the effect of the perturbing forces on the lengths of the semi-axes of the elliptic orbits around linearly stable triangular points.

The panel (a) describes the difference in the lengths of the semi-axes of the elliptic orbits for the classical model (inner path) and when the problem is modeled to include oblateness of the primary star (outer path). The diagram in panel (b) compares the lengths of the semi-major and minor axes of the ellipse. The inner and outer path correspond to that of classical case and generalized model, respectively while the lengths of the axes for the classical problem, model with oblate primary star and the generalized model, are presented in panel (c). The last diagram in panel (d) is the combined plots of all the cases 1 to 17 in Table 7.

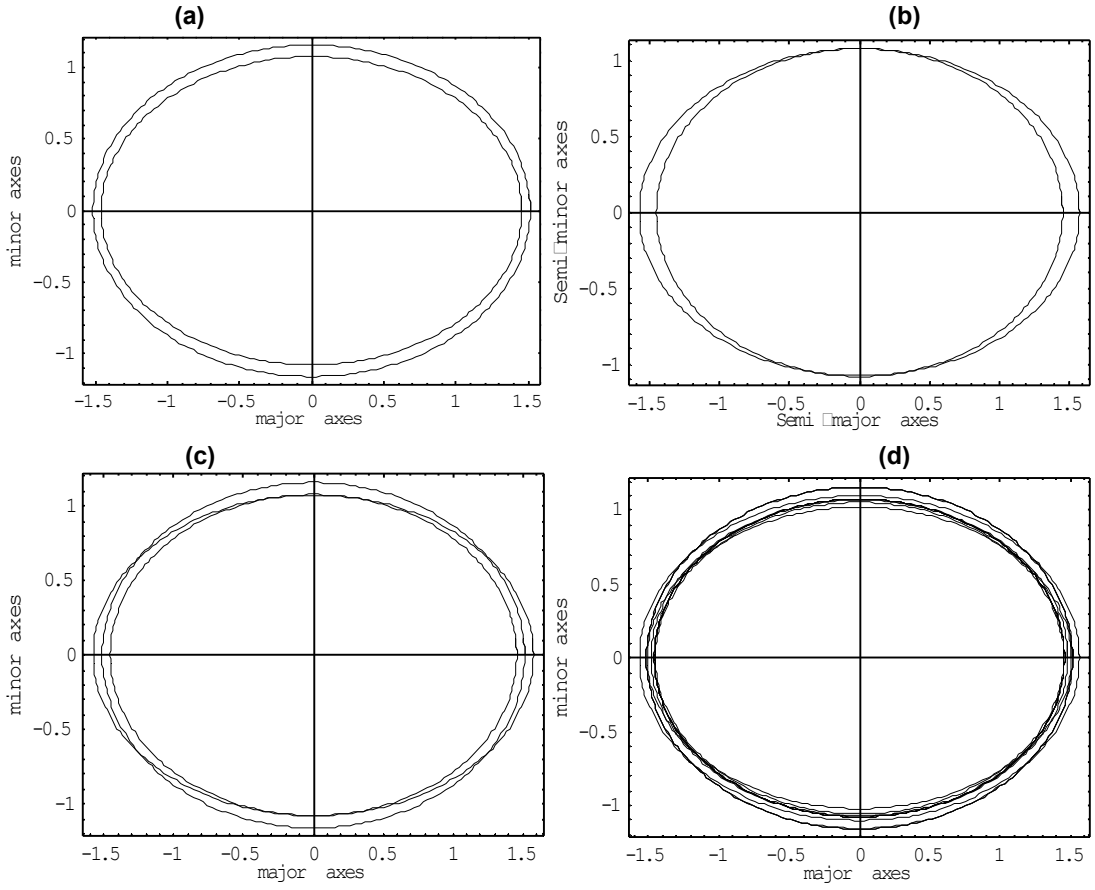

Fig. 6. Semi-major and minor axes of the elliptic orbits around triangular equilibria in the case of (a) classical model (inner path) and formulation with oblate bigger star (outer path) (b) classical model (inner) and generalized formulation (outer) (c) classical model (inner path), formulation with oblate primary star and generalized model (d) combined plots of all the different formulations

Table 7. Effect of perturbed forces on the eccentricity and semi-axes of the orbits

S/N	q_1	q_2	α_1	α_2	α_3	$\in$	$\in'$	M_d	e	a	b
1	1	1	0	0	0	0	0	0	0.30378	1.4589	1.0772
2	0.9988	1	0	0	0	0	0	0	0.30426	1.4595	1.0774
3	1	0.9985	0	0	0	0	0	0	0.30437	1.4586	1.0758
4	0.9988	0.9985	0	0	0	0	0	0	0.30485	1.4592	1.0760
5	1	1	0.024	0	0	0	0	0	0.51541	1.5145	1.1582
6	1	1	0	0.02	0	0	0	0	0.49371	1.5093	1.0219
7	1	1	0	0	0.015	0	0	0	0.35037	1.4818	1.0766
8	1	1	0	0	0	0.001	0	0	0.30378	1.4589	1.0772
9	1	1	0	0	0	0	0.002	0	0.31392	1.4578	1.0732
10	1	1	0	0	0	0	0	0.01	0.27636	1.4519	1.0551
11	0.9988	1	0.024	0	0	0	0	0	0.51588	1.5151	1.1584
12	0.9988	0.9985	0.024	0	0	0	0	0	0.51647	1.5148	1.1570
13	0.9988	0.9985	0.024	0.02	0	0	0	0	0.70640	1.5652	1.1016
14	0.9988	0.9985	0.024	0.02	0.015	0	0	0	0.75298	1.5880	1.1010
15	0.9988	0.9985	0.024	0.02	0.015	0.001	0	0	0.75298	1.5880	1.1010
16	0.9988	0.9985	0.024	0.02	0.015	0.001	0.002	0	0.76312	1.5869	1.0969
17	0.9988	0.9985	0.024	0.02	0.015	0.001	0.002	0.01	0.73570	1.5799	1.0748

Table 8. Effects of increase in mass of accumulated materials around the stars on the eccentricity, semi-axes and orientation of the elliptic orbits for $q_1 = 0.9988, q_2 = 0.9985, \alpha_1 = 0.024, \alpha_2 = 0.02, \alpha_3 = 0.015, \in = 0.001, \in' = 0.002$

M_d	e	a	b	α
0	0.76312	1.5869	1.0969	2.4208
0.001	0.76038	1.5862	1.0947	2.7448
0.005	0.74941	1.5834	1.0859	4.0331
0.009	0.73844	1.5806	1.0770	5.3052
0.01	0.73570	1.5799	1.0748	5.6201
0.02	0.70827	1.5729	1.0527	8.6839
0.03	0.68085	1.5659	1.0306	11.5562
0.04	0.65343	1.5590	1.0085	14.2028
0.05	0.62600	1.5520	0.9863	16.6095
0.06	0.59858	1.5450	0.9642	18.7780
0.07	0.57115	1.5380	0.9421	20.7208
0.08	0.54373	1.5310	0.9200	22.4561
0.09	0.51630	1.5240	0.8979	24.0047
0.099	0.49162	1.5177	0.8780	25.2558
0.0999	0.48915	1.5171	0.8760	25.3742

Table 9. Effects of potential of the cluster on elements of the elliptic orbits for $q_1 = 0.9988, q_2 = 0.9985, \alpha_1 = 0.024, \alpha_2 = 0.02, \alpha_3 = 0.015, \in = 0.001, \in' = 0.002$

T	e ($M_d = 0.01$ =0.02 =0.04)	a ($M_d = 0.01$ =0.02 =0.04)	b ($M_d = 0.01$ =0.02 =0.04)	α ($M_d = 0.01$ =0.02 =0.04)
0	0.735692	1.57998	1.07484	5.6211
	0.708259	1.57298	1.05272	8.6858
	0.653392	1.55899	1.00848	14.2060
0.0001	0.735692	1.57998	1.07484	5.6211
	0.708259	1.57298	1.05272	8.6858
	0.653392	1.55899	1.00848	14.2060
0.0005	0.735692	1.57998	1.07484	5.6211
	0.708259	1.57298	1.05272	8.6858
	0.653392	1.55899	1.00848	14.2060
0.001	0.735693	1.57998	1.07484	5.6211
	0.708259	1.57298	1.05272	8.6858
	0.653392	1.55899	1.00848	14.2060
0.002	0.735693	1.57998	1.07484	5.6211
	0.708259	1.57298	1.05272	8.6858
	0.653392	1.55899	1.00848	14.2060
0.005	0.735695	1.57998	1.07484	5.6211
	0.708264	1.57298	1.05272	8.6854
	0.653401	1.55899	1.00848	14.2052
0.009	0.7357	1.57998	1.07484	5.6203
	0.708274	1.57299	1.05273	8.6482
	0.653422	1.559	1.0085	14.2034
0.01	0.735702	1.57998	1.07485	5.6201
	0.708278	1.57299	1.05273	8.6879
	0.65343	1.559	1.0085	14.2028
0.02	0.73573	1.57999	1.07486	5.6171
	0.708335	1.57301	1.05277	8.6782
	0.653544	1.55904	1.00857	14.1932

Table 10. Deviations of the orbital elements from the classical case due to the perturbing forces

cases	Parameter forces	Frequency	Period	Angle of rotation	eccentricity	Semi-major	Semi-minor
1	q_1	Decreases	Increases	Increases	Increases	Increases	Increases
2	q_2	Decreases	Increases	Increases	Increases	Decreases	Decreases
3	α_1	Decreases	Increases	Increases	Increases	Increases	Increases
4	α_2	Decreases	Increases	Decreases	Increases	Increases	Decreases
5	α_3	Decreases	Increases	Increases	Increases	Increases	Decreases
6	φ	Decreases	Increases	No effect	No effect	No effect	No effect
7	ψ	Decreases	Increases	Decreases	Increases	Decreases	Decreases
8	M_d	Decreases	Increases	Increases	Decreases	Decreases	Decreases
1 and 2		Decreases	Increases	Increases	Increases	Increases	Decreases
1,2 and 3		Decreases	Increases	Increases	Increases	Increases	Increases
1,2,3,4		Decreases	Increases	Increases	Increases	Increases	Increases
1,2,3,4,5		Decreases	Increases	Increases	Increases	Increases	Increases
1,2,3,4,5,6		Decreases	Increases	Increases	Increases	Increases	Increases
1,2,3,4,5,6,7		Decreases	Increases	Increases	Increases	increases	increases
1,2,3,4,5,6,7,8		Decreases	Increases	Increases	Increases	Increases	Decreases

Table 8, provides numerical evidence that an increase in mass of accumulated materials around the stars result in a decrease in the eccentricity, and lengths of the semi-axes while it increases the angle of rotation of the principal axis. The same result is also seen in Table 9 below, where we take into account effects of the density profile of the circular cluster of material points on the eccentricity, semi-axes and the angle of rotation of the principal axis.

Finally, from our numerical efforts we can weigh the deviations of the frequency, angle of rotation, period, eccentricity and lengths of the semi-axes from the classical numerical estimations due to the effect of the perturbing forces. We give this in a tabular form in Table 10 for easy understanding.

Here the increase or decrease is a measure of the deviation from the classical estimations.

5. DISCUSSION AND CONCLUSION

The analytical and numerical investigation of effect of perturbing forces on periodic orbits around linearly stable triangular equilibrium points of the RTBP has been carried out when motion of an oblate infinitesimal mass takes place in the presence of cluster of material, small perturbations in the Coriolis and centrifugal forces, radiation pressure and oblateness of the primaries. This is a generalized study of researches performed by Singh and Haruna [12], Singh and Leke [13], Abouelmagd and EL–Shaboury [11], AbdulRaheem and Singh [9], Perdios and Kalantonis [8], Perdios [7] and several others. Clearly, the equations of motion of this study and those of Singh and Haruna [12] differ because of the potential of the circular cluster of material points which we have included in this investigation, while the difference between these equations and those given in AbdulRaheem and Singh [9] are due to oblateness of the infinitesimal mass and potential from the cluster. The same differences are seen in the coordinate of the triangular equilibrium points. Now, equations (6) and (7) give the equations of the frequencies for the long and short period orbits, respectively. These equations have an additional term due to the cluster around the primaries which does not appear in the obtained expression for the frequency of the long period orbits calculated in Singh and Haruna [12]. However, in the absence of the circular enclosure, these expressions fully coincide. They however differ from those found in AbdulRaheem and Singh [9], not only because of the inclusion that the infinitesimal mass has the shape of an oblate spheroid and the primaries enclosed by accumulated materials but also in the coefficients of the oblateness of the more massive primary.

Equation (17) gives the angle of rotation of the principal axis of the elliptic orbits in terms of the parameters, representing the radiation pressure of the stars, oblateness of the bodies, cluster of materials and small perturbation in the centrifugal force. The Coriolis perturbation has no effect on how the axes are oriented. Equation (17) shows that the orientation of these orbits may increase or decrease. This will depend on the parameters of the system. If an increase or decreases occur, then this will produce a change in the orientation of the orbits along the $\bar{\xi}$ coordinate. This equation (17) coincides with that in the absence of cluster of materials fully coincide with the one in Singh and Haruna [12] Some of the coefficients of the system parameters of our problem are same with some in AbdulRaheem and Singh [9], except for what seems like a typographic error in the coefficient of the oblateness of the more massive star, this error was also spotted in the paper by Singh and Haruna [12].

The eccentricity of the elliptic orbit given in equation (22) depends on the system parameters except the small perturbation in the Coriolis force, and differs from that in Singh and Haruna [12] and AbdulRaheem and Singh [9]. It should be noted that the coefficients of the radiation factors in (22) are different from those in Singh and Haruna [12]. The lengths of the semi-axes have been calculated in equations (24) and (25). It is seen that the lengths are not affected by the Coriolis perturbation and differ from those of previous studies due to the presence of cluster of matters around the stars. We observed that these lengths and those in Singh and Haruna [12] have some terms which fully coincide and some which do not; for instance, the coefficients of the radiation factors.

Finally, from our numerical explorations of the problem which is interpreted in Table 10, we can make the following statements that:

i. All perturbing forces reduces angular frequency
ii. All perturbing forces increases time period

iii. Radiation pressure of the bigger star increases angle of rotation of principal axis, eccentricity and lengths of the semi-major and semi-minor axes of the orbits,
iv. Radiation pressure of the smaller star increases angle of rotation and eccentricity but reduces lengths of both semi-axes.
v. When both stars are radiating spherical bodies, lengths of semi-major axis increases while the minor-axis decreases,
vi. Oblateness of the bigger star increases angle of rotation, eccentricity and lengths of semi-axes of the orbits,
vii. Oblateness of the smaller star increases eccentricity and length of semi-major axis but reduces angle of rotation and length of minor axis.
viii. Oblateness of infinitesimal mass increases angle of rotation, eccentricity and length of major axis but reduces length of minor axis.
ix. Presence of the cluster of material points increases angle of rotation but reduces eccentricity and lengths of semi-axes.
x. In the presence of oblateness of the bigger star and absence of cluster, the semi axes increase always.
xi. Small perturbation in the Coriolis force does not affect angle of rotation, eccentricity and lengths of semi-axes
xii. Small centrifugal perturbation increases eccentricity but reduces angle of rotation and lengths of the semi-axes.
xiii. Of all the perturbing forces only cluster of materials reduces eccentricity.
xiv. Radiation pressure and oblateness of the bigger star have same effect on the structure of the orbits.
xv. Under combined effect of the perturbing forces, the period, angle of rotation, eccentricity and length of semi-major axis all increases, while frequency and length of semi-minor axis reduces.

These facts are not directly observable from the analytic solutions obtained except (xi).

Our study has relevance in motion of planets around binary systems, where planets have masses infinitesimally small. A simple question of celestial mechanics is: how long can the triangular equilibrium points keep the infinitesimal mass in orbit from escaping? The determination of ranges of semi-major axis taking into account the perturbing forces may help to know if body is likely to remain or escape. Now, since under combined effect of the perturbing forces, the period, angle of rotation, eccentricity and length of semi-major axis all increases, we conclude the infinitesimal mass is likely to escape under the combined effect of radiation, perturbations, oblateness and cluster of materials. However, with increasing accumulation of materials, the infinitesimal mass will remain in orbit around the triangular points as its effect will override other perturbing forces and reduce the length of the semi-major axis.

COMPETING INTERESTS

Authors have declared that no competing interests exist.

REFERENCES

1. Shpenkov GP. Dialectical view of the world: The wave model (Selected Lectures). Dynamic Model of Elementary Particles, Part 1. Fundamentals, Lecture. 2013;6(3):63-65.
2. Christianto V. Comparison of predictions of planetary quantization and implications of the Sedna finding. Apeiron. 2004; 11(3):82–98.
3. Szebehely VG. Theory of Orbits, Academic Press, New York; 1967.
4. Krasnoholovets V. Structure of space and the submicroscopic deterministic concept of physics, Apple Academic Press. Chapter 8; 2017.
5. Zagouras CG. Periodic motion around the triangular equilibrium points of the photo–gravitational restricted problem of three bodies. Celestial Mechanics and Dynamical Astronomy. 1991;51:331.
6. Elipe A, Lara M. Periodic orbits in the restricted three-body problem with radiation pressure. Celestial Mechanics and Dynamical Astronomy. 1997;68:1
7. Perdios EA. Critical symmetric periodic orbits in the photogravitational restricted three-body problem. Astrophysics and Space Science. 2003;286:501.
8. Perdios EA, Kalantonis VS. Critical periodic orbits in the restricted three- body problem with oblateness. Astrophysics and Space Science. 2006;305:331.
9. AbdulRaheem A, Singh J. Combined effects of perturbations, radiation and oblateness on the periodic orbits in the restricted three-body problem. Astrophysics and Space Science. 2008; 317:9.

10. Mittal A, Ahmad I, Bhatnagar KB. Periodic orbits generated by Lagrangian solutions of the restricted three-body problem when one of the primaries is an oblate body. Astrophysics and Space Science. 2009; 319:63.
11. Abouelmagd EI, EL–Shaboury SM. Periodic orbits under combined effects of oblateness and radiation in the restricted problem of three bodies. Astrophysics and Space Science. 20121;341:331.
12. Singh J, Haruna S. Periodic orbits around triangular points in the restricted problem of three oblate bodies. American Journal of Astronomy and Astrophysics. 2014;2: 22.
13. Singh J, Leke O. Periodic orbits in the Chermnykh-like restricted problem of oblate bodies with radiation. Astrophysics and Space Science. 2014a;350:109.
14. Singh J, Leke O. Effects of mass variation of main bodies on orbits around triangular libration points in the restricted three-body problem. Journal of Applied Physical Science International. 2014b;1:10.
15. Palacios M, Arribas M, Abad A, et al. Symmetric periodic orbits in the Moulton Copenhagen problem. Celestial Mechanics and Dynamical Astronomy. 2019;131:16.
16. Johnson A, Sharma RK. Locations of Lagrangian points and periodic orbits around triangular points in the photo gravitational elliptic restricted three-body problem with oblateness. International Journal of Advanced Astronomy. 2019;7:25.
17. Mittal A, Suraj MS, Aggarwal R. Periodic orbits generated by Lagrangian solutions of the restricted three-body problem with non-spherical primaries. New Astronomy; 2020.
18. Wolfram S. The Mathematica Book, 10th Ed. Wolfram Media, Campaigns; 2017.

Peer-review history:
The peer review history for this paper can be accessed here:
http://www.sdiarticle4.com/review-history/62848